Determination of the Charge State Distribution of a Highly Ionized Coronal Au Plasma

K. L. Wong, M. J. May, P. Beiersdorfer, K. B. Fournier, B. Wilson, G. V. Brown, and P. Springer
Lawrence Livermore National Laboratory, P.O. Box 808, Livermore, California 94551, USA

P. A. Neill and C. L. Harris
Department of Physics, University of Nevada Reno, Reno, Nevada 89557, USA
(Received 16 April 2002; published 10 June 2003)

We present the first definitive measurement of the charge state distribution of a highly ionized gold plasma in coronal equilibrium. The experiment utilized the Livermore electron beam ion trap EBIT-II in a novel configuration to create a plasma with a Maxwellian temperature of 2.5 keV. The charge balance in the plasma was inferred from spectral line emission measurements which accounted for charge exchange effects. The measured average ionization state was 46.8 ± 0.75. This differs from the predictions of two modeling codes by up to four charge states.

DOI: 10.1103/PhysRevLett.90.235001 PACS numbers: 52.20.Fs, 52.25.Jm

Predicting the correct charge state distribution is critical for understanding radiation levels, energy deposition, energy balance, etc. of high temperature plasmas such as those produced inside Z pinches [1,2], tokamaks [3,4], astrophysical objects [5], and hohlraums irradiated by intense lasers [6–9]. Reasonable predictions from models can be obtained for the charge state distribution (CSD) of low-Z elements in the nonlocal thermodynamic equilibrium (NLTE) plasma [10,11]. However, these models are far from adequate to predict the charge state distribution for high-Z elements in the NLTE plasma. This inadequacy has been strikingly illustrated in a comparison of recent NLTE calculations of the charge state distribution of several elements [11]. The calculations for high-Z elements at conditions of typical laser-produced plasmas had the most significant discrepancies: For example, the predicted average charge state, $\langle q \rangle$, for gold at a temperature $T_e = 2.5$ keV and a density $n_e = 10^{20}$ cm^{-3} varied from +43 to +63. The models require several definitive experiments to test their implementation of the atomic physics processes. Such experiments need to be performed at various plasma conditions in order to isolate and study specific atomic physics processes. In particular, the low-density plasmas have fewer active relevant processes (e.g., no photoionization, opacity, three-body recombination, etc.) and also provide less complicated experiments than the high-density ones.

Recently, two high-density experiments with different plasma conditions have been done with the NOVA laser to determine the ionization balance of Au. Foord [12] inferred the charge state balance of a heated gold microdot buried in a Be foil at $n_e = 6 \times 10^{20}$ cm^{-3} and $T_e = 2.2$ keV in steady state by comparing the measured spectrum with atomic physics calculations. The experimental $\langle q \rangle = +49.3 \pm 0.5$ was in reasonable agreement with the modeled value of +49.1 from RIGEL/MCXSN [13]. To reproduce properly the experiment, two-electron processes such as dielectronic recombination were included in the modeling of the charge balance and the line brightnesses. Glenzer [14] measured the average gold ion charge state to be $+52 \pm 1$ in a fusion hohlraum plasma with T_e of 2.6 keV, n_e of 1.4×10^{21} cm^{-3}, and a soft x-ray radiation temperature of 210 eV. The predicted steady state $\langle q \rangle = +50.5$ which was also calculated by RIGEL/MCXSN was just outside the experimental error bar. Glenzer indicated that nonsteady state kinetics might be a possible explanation of the discrepancy. The analysis of these high-density experiments was complicated by the transient nature of the laser-produced plasma and the many competing atomic processes present in these plasmas.

In this Letter, we present the first definitive experimental determination of the charge balance of gold in coronal conditions. This has been possible with the development of two experimental techniques. First, we have used an experimentally simulated thermal electron distribution to create an equilibrium charge state balance. Second, we have developed a procedure utilizing the magnetic trapping mode [15] that addresses the effect of charge exchange with the background gas in an electron beam ion trap [16,17]. The Livermore EBIT-II device was used to create the gold plasma with a Maxwell-Boltzmann temperature of 2.5 keV and an electron density of $\approx 10^{12}$ cm^{-3}. The charge balance was inferred by comparing the gold x-ray emission line intensities with atomic physics calculations from the Hebrew University Lawrence Livermore Atomic Code (HULLAC) [18]. These measurements observe the ionization balance in steady state conditions. Despite the simplification afforded by the coronal plasma, the inferred charge state distribution from EBIT-II disagrees with the results from the available modeling codes.

The gold plasma in EBIT-II was produced by successive electron collisional ionization of low-charged ions

introduced into the trap from a metal vacuum vapor ion source [19]. In the electron mode [15], the ions were trapped radially by the monoenergetic electron beam and axially along the beam by two end drift tubes which have a positive bias of a few hundred volts with respect to a center drift tube. The gold particles ionized for about 50 ms during which time the electron beam was kept at a constant energy of 2.2 keV. Then, the electron beam energy and anode voltage were swept to map out a Maxwell-Boltzmann electron distribution in time with a temperature of 2.50 ± 0.04 keV by using the techniques described in Ref. [20]. In each sweep, the time spent at an electron beam energy was proportional to the 2.5 keV Maxwell-Boltzmann electron distribution probability at that energy. The beam energy was swept in 256 discrete voltage steps between electron energies of 200 to 12 500 eV. Concurrently, the anode voltage was appropriately swept to maintain a constant density in the electron beam. The sweep was 5 ms in duration and was continuously repeated until the end of the electron mode. We monitored the time history of the Au x-ray emission to check when it came into steady state, which was after about 1 sec. The Au ions were held in the trap and interacted with the Maxwell-Boltzmann electron beam for another 6 sec for the charge state distribution measurements. Subsequently, the electron beam was turned off and the ions were trapped by the 3 T axial magnetic field in the magnetic mode [15] for an additional 6 sec in order to measure the effect of charge exchange. The trapping cycle was repeated for a total data acquisition time of $\sim$12 h for a complete charge balance measurement. This time was necessary to gain sufficient signal in the x-ray spectra collected in the magnetic and electron modes. More than a dozen charge balance measurements were performed to collect the data presented in this Letter.

The x-ray emission was measured through radial ports in the center drift tube by a solid-state Ge detector and a high-resolution flat crystal x-ray spectrometer [21]. The spectrometer utilized a Si(111) crystal with a lattice spacing of $2d = 6.271$ Å set to a nominal Bragg angle of 36°. The total coverage of the spectrometer was roughly 500 eV with a spectral resolution of about 5 eV. A raw Au spectrum taken during the Maxwell-Boltzmann sweeps is shown in Fig. 1. The M-shell lines are produced from pairs of $5f_{5/2} \rightarrow 3d_{3/2}$ and $5f_{7/2} \rightarrow 3d_{5/2}$ transitions in Ni-like through Br-like ions of Au. The $5f_{5/2} \rightarrow 3d_{3/2}$ transition is the higher energy transition of each pair. The photon energy calibration was done with the well-known lines of $\mathrm{Ly}_{\alpha 1,2}$ in H-like Ar and the w transition in He-like Ar. A sharp falloff in the efficiency of the flat crystal spectrometer occurred at 3210 eV due to the Ar K absorption edge in the P10 gas of the proportional counter used as the detector. This was taken into account when the experimental spectrum was compared with the modeling. An absolute calibration was not necessary, as we normalized the total number of gold ions in the trap to unity for each charge balance measurement.

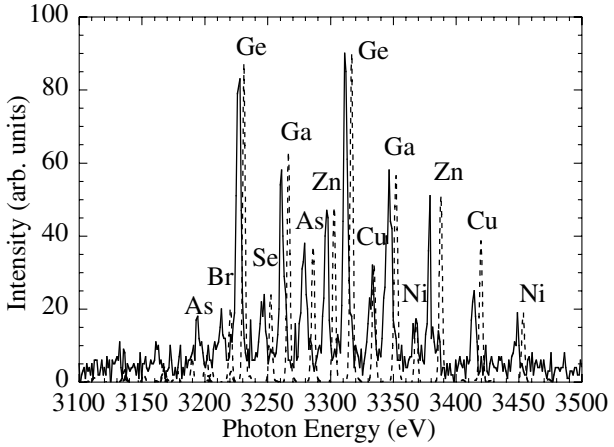

FIG. 1. Gold emission spectrum produced by a 2.5 keV experimentally simulated Maxwell-Boltzmann temperature in EBIT-II. For each charge state, the higher energy transition corresponds to a $5f_{5/2} \rightarrow 3d_{3/2}$ transition and the lower energy to a $5f_{7/2} \rightarrow 3d_{5/2}$ transition. Dashed lines are the HULLAC fits which are used to infer the charge state distribution.

The charge state distribution of the Au plasma was determined by individually fitting the intensity of the $5f \rightarrow 3d$ emission lines of each charge state with the simulated spectra from the HULLAC atomic data package calculated at $T_e = 2.5$ keV and $n_e = 1 \times 10^{12}$ cm^{-3}. HULLAC calculated the collisional cross sections and radiative decay rates to produce a spectrum for each charge state. It did not assume nor did it calculate any CSD. The fitted HULLAC spectrum which included the corrections for the spectrometer photometric sensitivity is shown in Fig. 1. The atomic transition rates and energy level structure of each ion were calculated from the Dirac equation with a parametric potential. Electron impact excitation cross sections were calculated in the distorted wave approximation. The HULLAC x-ray transition energies do not match the measured energies but differ by 3–10 eV, which illustrates the accuracy of the transition energy calculations. The level populations of each charge state were coupled with those of the adjacent higher-charged ion. The model for the higher-charged ion included fewer levels than the lower-charged ion and was considered only to include the effect of dielectronic recombination on the line brightnesses. In the EBIT-II plasma, collisional electron excitation from the ground level or metastable levels was the only significant process to populate an upper level. HULLAC calculations indicated that only one of the ions considered, Br-like, contained a significant electron population of more than 5% in metastable levels; that is, 10% of the Br-like ions (ground state: $3d^{10}4s^2 4p_{1/2}^2 4p_{3/2}^3 J = \frac{3}{2}$) were predicted to be in the metastable level $3d^{10}4s^2 4p_{1/2}^2 4p_{3/2}^2 4d_{3/2}$ $(J = \frac{7}{2})$. The

charge state distribution analysis included corrections to the line intensities due to the presence of the metastable states and ionization from the metastable states.

Figure 2 presents the experimental EBIT-II charge state distribution. Each point is the ionic fraction derived from the fit of the HULLAC intensities to one or two experimental lines. The error that brackets each point included the statistical error from the counts in the spectral lines and the uncertainty in the fit to the line or lines in each charge state. The line brightnesses calculated by HULLAC are assumed not to have any intrinsic error. The experiment is compared with the simulations from the available modeling codes: RIGEL/MCXSN, RIGEL/ENRICO, and the multiple ionization state transport (MIST) [23] code. RIGEL is typically used for high-density laser heated plasma experiments and is a super-configuration-based collisional-radiative code and solves for a CSD by using Monte Carlo techniques. MCXSN generates atomic physics rates for RIGEL based on hydrogenic supershells. ENRICO solves the Dirac equation explicitly to compute the radiative recombination and Auger processes: The collisional processes are calculated using generalized formulas. MIST is a low-density (10^{12} to 10^{14} cm^{-3}) tokamak impurity transport code and utilized the average ion model for the basis of its atomic physics rates [24]. Inclusion of the excitation-autoionization rates of Mitnik *et al.* [22] in MIST for charge states more highly ionized than Kr-like ions produced the dip in the charge balance at Kr-like Au. The

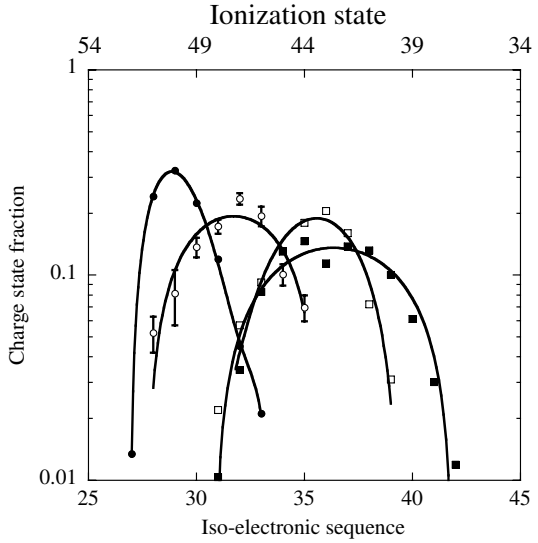

FIG. 2. Comparison of the gold charge state distribution at 2.5 keV determined from EBIT-II (open circle) and compared to the results from RIGEL/MCXSN (solid circle), RIGEL/ENRICO (open squares), and MIST (solid squares). The lines are added only to guide the eye. The dip at the Kr-like ion in the MIST charge balance is due to the inclusion of the excitation-autoionization rates of Mitnik *et al.* [22] missing in the lower charge states.

codes have been run with $n_e = 1 \times 10^{12}$ cm^{-3} and $T_e = 2.5$ keV. The calculations bracket the experiment. The average experimental charge state we found for the data in Fig. 2 was 47.4 ± 1.2. MIST predicted a lower average charge state by 4. RIGEL/MCXSN and RIGEL/ENRICO predicted a higher and lower average charge state by 3. Even by using the better implementation of atomic physics in RIGEL/ENRICO, a better calculation of the CSD is not obtained.

The charge balance in low-density laboratory plasmas can be affected by charge exchange with neutrals [25]. In order to test for the effect of charge exchange on the charge state distribution in EBIT-II, we repeated our measurements with different concentrations of background gas. We systematically varied the amount of Ar gas in the trap during a series of Au charge balance measurements by utilizing a gas injector with a precise continuous flow. The rate coefficient for charge exchange was measured during the magnetic mode utilizing the fact that the charge exchange produced x-ray emission proportional to the amount of neutral gas density, n_0 [26]. In the magnetic mode, the x-ray signal induced by the charge exchange decayed exponentially as the ions recombined. The exponential decay was determined by the charge exchange rate, $R_{CX} = n_0\langle v_0 \sigma_{CX}\rangle$, where v_0 is the neutral gas velocity and σ_{CX} is the charge exchange cross section of neutral argon with highly charged Au ions. Fitting the exponential decay of the x-ray signal yielded R_{CX} for the different amounts of neutral Ar gas. The average charge state inferred from the electron mode is plotted as a function of the charge exchange rate in Fig. 3. The uncertainties in the average charge state were calculated as discussed above. The uncertainties in the recombination rate (i.e., the exponential fit) were much smaller than the size of the symbols used in the figure. Within these uncertainties, the average charge state does not depend on charge exchange.

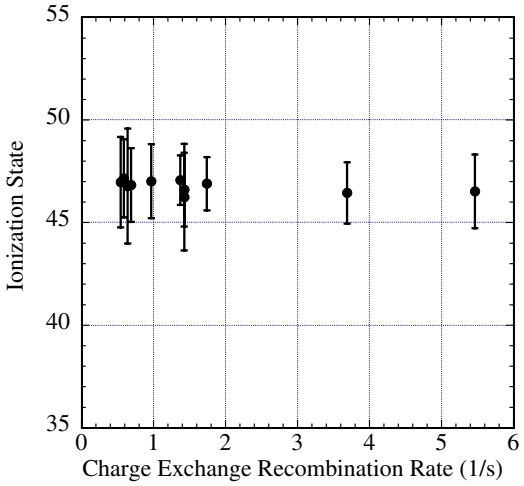

FIG. 3 (color online). The average charge of the Au plasma at 2.5 keV versus the charge exchange rate, R_{CX}.

TABLE I. Average charge state determined in coronal equilibrium on EBIT-II and calculations.

Source	Average charge state
EBIT-II	46.8 ± 0.75
RIGEL/MCXSN	49.5
RIGEL/ENRICO	43.7
MIST	42.7

Averaging over a dozen charge balance measurements each with a different amount of neutral gas density, we find a $\langle q \rangle$ of 46.8 ± 0.75. The final uncertainty results from the sum of the uncertainties in each measurement and from the accuracy with which the effects of charge exchange could be determined. The results are summarized in Table I and compared with the $\langle q \rangle$ values predicted by the MIST and RIGEL calculations.

In conclusion, we presented the first definitive measurement of the Au charge state balance in an experimentally simulated thermal plasma having a temperature of 2.5 keV in coronal conditions. The x-ray emission from the $5f \rightarrow 3d$ transitions from M-shell Au was compared with line emission calculations from HULLAC to infer the charge balance. The $\langle q \rangle$ of 46.8 ± 0.75 that was obtained from the average over our approximately dozen measurements was in disagreement with the predicted $\langle q \rangle$ from the RIGEL and the $\langle q \rangle$ of 42.7 from the MIST code. Despite the steady state conditions and simpler atomic physics in the EBIT plasma, the available modeling codes do not adequately reproduce the measurement. This disagreement demonstrates the need for more experiments. Furthermore, our differences when using the predictions of RIGEL are larger than those found in the high-density experiments [12,14] and are more consistent with those from Ref. [11] which indicates that ionization balance calculations do not yet have the predictive power necessary to describe the ionization equilibrium of an arbitrary plasma.

This work was performed under the auspices of the U.S. Department of Energy by the University of California Lawrence Livermore National Laboratory under Contract No. W-7405-ENG-48.

[1] K. L. Wong, P. T. Springer, J. H. Hammer, C. A. Iglesias, A. L. Osterheld, M. E. Foord, H. C. Bruns, and J. A. Emig, Phys. Rev. Lett. **80**, 2334 (1998).
[2] A. L. Velikovich, J. Davis, V. I. Oreshkin, J. P. Apruzese, R. W. Clark, J. W. Thornhill, and L. I. Rudakov, Phys. Plasmas **8**, 4509 (2001).
[3] C. De Michelis and M. Mattioli, Rep. Prog. Phys. **47**, 1233 (1984).
[4] J. E. Rice, J. L. Terry, K. B. Fournier, M. A. Graf, M. Finkenthal, M. J. May, E. S. Marmar, W. H. Goldstein, and A. E. Hubbard, J. Phys. B **29**, 2191 (1996).
[5] J. C. Raymond and N. S. Brickhouse, Astrophys. Space Sci. **237**, 321 (1996).
[6] H. R. Griem, Phys. Fluids B **4**, 2346 (1992)
[7] J. Lindl, Phys. Plasmas **2**, 3933 (1995).
[8] M. Fajardo, P. Audebert, P. Renaudin, H. Yashiro, R. Shepherd, J. C. Gauthier, and C. Chenais-Popovics, Phys. Rev. Lett. **86**, 1231 (2001).
[9] C. Y. Côté, J. C. Kieffer, and O. Peyrusse, Phys. Rev. E **56**, 992 (1997).
[10] A. Hauer, K. G. Whitney, P. C. Kepple, and J. Davis, Phys. Rev. A, **28**, 963 (1983).
[11] R. W. Lee, J. K. Nash, and Y. Ralchenko, J. Quant. Spectrosc. Radiat. Transfer **58**, 737 (1997).
[12] M. E. Foord, S. H. Glenzer, R. S. Thoe, K. L. Wong, K. B. Fournier, B. G. Wilson, and P. T. Springer, Phys. Rev. Lett. **85**, 992 (2000).
[13] B. G. Wilson *et al.*, *Radiative Properties of Hot Dense Matter*, edited by W. Goldstein, C. Hooper, J. Gauthier, J. Seely, and R. Lee (World Scientific, Singapore, 1991).
[14] S. H. Glenzer, K. B. Fournier, B. G. Wilson, R. W. Lee, and L. J. Suter, Phys. Rev. Lett. **87**, 045002 (2001).
[15] P. Beiersdorfer, L. Schweikhard, J. Crespo Lopez-Urrutia, and K. Widmann, Rev. Sci. Instrum. **67**, 3818 (1996).
[16] M. A. Levine, R. E. Marrs, J. R. Henderson, D. A. Knapp, and M. B. Schneider, Phys. Scr., T **22**, 157 (1988).
[17] R. Marrs, P. Beiersdorfer, and D. Schneider, Phys. Today **47**, 27 (1994).
[18] A. Bar-Shalom, M. Klapisch, and J. Oreg, J. Quant. Spectrosc. Radiat. Transfer **71**, 169 (2001).
[19] I. G. Brown, J. . Galvin, R. A. MacGill, and R. T. Wright, Appl. Phys. Lett. **49**, 1019 (1986).
[20] D. W. Savin, P. Beiersdorfer, S. M. Kahn, B. R. Beck, G. V. Brown, M. F. Gu, D. A. Liedahl, and J. H. Scofield, Rev. Sci. Instrum. **71**, 3362 (2000).
[21] G. V. Brown, P. Beiersdorfer, and K. Widmann, Rev. Sci. Instrum. **70**, 280 (1999).
[22] D. Mitnik, P. Mandelbaum, J. L. Schwob, A. Bar-Shalom, J. Oreg, and W. H. Goldstein, Phys. Rev. A **50**, 4911 (1994).
[23] R. A. Hulse, Nucl. Technol. Fusion **3**, 259 (1983).
[24] D. E. Post, J. V. Jensen, C. B. Tarter, W. H. Grasberger, and W. A. Lokke, At. Data Nucl. Data Tables **20**, 397 (1977).
[25] R. A. Hulse, D. E. Post, and D. R. Mikkelsen, J. Phys. B **13**, 3895 (1980).
[26] P. Beiersdorfer, R. E. Olson, G. V. Brown, H. Chen, C. L. Harris, P. A. Neill, L. Schweikhard, S. B. Utter, and K. Widmann, Phys. Rev. Lett. **85**, 5090 (2000).